energies

MDPI

Article

Geochemical Characteristics of the Chang 7 Source Rocks of the Triassic Yanchang Formation in Ordos Basin, China: Implications for Organic Matter Accumulation and Shale Oil Potential

Lewei Hao [1], Xiaofeng Ma [1,*], Wenqiang Gao [1,2,*], Zhaocai Ren [3], Huifei Tao [1] and Weikai Huang [1,4]

[1] Key Laboratory of Petroleum Resources, Northwest Institute of Eco-Environment and Resources, Chinese Academy of Sciences, Lanzhou 730030, China
[2] Bailie School of Petroleum Engineering, Lanzhou City University, Lanzhou 730070, China
[3] Exploration and Development Research Institute of PetroChina Changqing Oilfield Company, Xi'an 710018, China
[4] University of Chinese Academy of Sciences, Beijing 100049, China
* Correspondence: maxf@lzb.ac.cn (X.M.); gaowq726@163.com (W.G.)

Abstract: The Chang 7 member of the Upper Triassic Yanchang Formation in the Ordos Basin is considered to hold the main source rocks for conventional and unconventional oil and gas. The lamination or lithology alteration in vertical and lateral directions, even over a short distance, is a common feature in lacustrine source rocks. The differences in the geochemical characteristics of black shales, dark mudstones and interbedded sandstones have been scarcely reported, and their influences on the petroleum generation potential and shale oil potential are not clear. To this end, 22 core samples were collected from the Lower and Middle Chang 7 (C7-3 and C7-2) members of the Triassic from well CYX in the Qingcheng area. By conducting a series of geochemical analyses including TOC, Rock-Eval pyrolysis yields, bitumen extraction and quantification, and the separation and quantification of saturates, aromatics, resins and asphaltenes, along with biomarker analyses, several results were found. Firstly, the C7-3 and C7-2 source rocks are thermally mature and have entered into the stage of hydrocarbon generation. The C7-3 and C7-2 source rocks have a good to very good hydrocarbon generation potential especially the C7-3 black shales. Secondly, terrigenous source input is more abundant in C7-2, whereas the source input of phytoplankton, algae or microbial lipids is more abundant in C7-3. Moreover, a high TOC content basically corresponds to low wax indexes, terrigenous/aquatic ratios (TARs), and Pr/nC_{17} and Ph/nC_{18} ratios and high C_{27}/C_{29} regular sterane ratios, which suggests that the source input of phytoplankton, algae or microbial lipids is favorable for OM accumulation. Third, analyses of the molecular composition of saturated fractions in shales and interbedded sandstones and the production index demonstrate the migration of petroleum from organic-rich source rocks to their organic-lean counterparts. The C7-2 dark mudstones could be considered as a potential "sweet spot" since their oil saturation index (OSI) was the highest among all the studied samples and they are more enriched in light aliphatic fractions.

Keywords: source rocks; organic matter accumulation; shale oil potential; Yanchang Formation; Ordos Basin

Citation: Hao, L.; Ma, X.; Gao, W.; Ren, Z.; Tao, H.; Huang, W. Geochemical Characteristics of the Chang 7 Source Rocks of the Triassic Yanchang Formation in Ordos Basin, China: Implications for Organic Matter Accumulation and Shale Oil Potential. *Energies* **2022**, *15*, 7815. https://doi.org/10.3390/en15207815

Academic Editors: Bei Liu, Tian Dong, Wenhao Li, Kun Jiao and Zhen Qiu

Received: 19 September 2022
Accepted: 19 October 2022
Published: 21 October 2022

1. Introduction

Source rocks containing abundant organic matter (OM) generate a large amount of oil and gas during thermal maturation and lay the foundation for petroleum systems [1–3]. Amid the development the of petroleum industry and rising demands for oil and gas in recent years, to reduce exploration risks, the factors controlling OM enrichment in source rocks have long been one of the main issues for petroleum geologists [4–8]. According to previous studies, several factors that govern the formation of OM-rich source rocks have

been proposed [9–12]. First, a high flux of organic matter to the sediment is needed, which ultimately depends on a high rate of biological productivity [13–16]. Second, OM can be oxidized by oxidants and lead to the combustion of OM, so the availability of oxidants, and particularly oxygen, is a crucial factor in the survival of OM. The limited amounts of oxygen in the water column or anoxic depositional environments favor the formation of OM-rich sediments [17–20]. Third, the sedimentation rate is another important factor that affects the preservation of OM. The sedimentation rate's influence on the accumulation of OM is complicated. Specifically, a high sedimentation rate leads to quick burial, thus reducing OM consumption or the dilution of OM as a result of the excessive clastic source input [21,22]. Instead, a slow sedimentation rate results in bioturbation and the oxidation of OM, as well as absence of OM dilution [23]. Other important factors include the type of water column (i.e., upwelling, downwelling and stratification), sea level effect, rate of precipitation, fluviatile input, and weathering intensity [11]. However, the formation of source rocks with abundant OM is generally the result of comprehensive factors [9,11].

One common feature of lacustrine source rocks is the lamination or lithology alteration in vertical and lateral directions due to the frequent changes in the depositional environment, water condition and provenance [24]. This, in turn, results in source rocks with contrasting total organic carbon (TOC) contents during the evolution of the lake basin. Taking the Ordos Basin as an example, which is the second largest petroleum-bearing basin in China, a number of suits of source rocks have developed in the Upper Triassic Yanchang Formation. Among these source rocks, the Chang 7 member (C7) is mainly composed of organic-rich shales and mudstones, with the highest TOC content, on average, compared with other members; thus, it is considered to hold the main source rocks in the basin. The C7 source rocks were deposited in a semi-deep to deep water environment during the period when the lake expanded to its peak value [25–27]. However, the lithologies and OM enrichment of the C7 source rocks changed laterally and vertically, even over a short distance. The heterogeneity of the TOC content gives rise to questions concerning what factors have controlled the accumulation of OM. In addition to the three primary factors mentioned above, i.e., productivity, anoxic depositional environment and sedimentation rate, a number of studies have suggested that volcanic and hydrothermal activities may play a significant role in OM accumulation [4]. However, the factors that control OM accumulation and the reasons why source rocks with variable TOC contents developed during the deposition of the Yanchang Formation still remain controversial and are not well-known.

Recently, since the development of volume fracturing technology for horizontal well, it has been shown that these organic-rich shales or mudstones can act not only as source rocks for conventional petroleum but also as important reservoirs for unconventional oil and gas (shale oil and gas or tight oil and gas). The differences in OM enrichment basically may cause variations in the richness or quality of the source rocks, which in turn has a significant effect on the petroleum generation potential. Thus, figuring out the differences in thr geochemical characteristics of these source rocks is crucial for conventional and unconventional oil and gas exploration and exploitation. Previous studies commonly divided source rocks of the Chang 7 member into black shales and dark mudstones, and many works have been done on observing the geochemical characteristics of two kinds of source rocks [28,29]. According to thermal maturity, petroleum potential and organic matter type, the shales have a better hydrocarbon generation potential than the mudstones [28,29]. The paleoenvironments of mudstones and shales show reducing to sub-oxidizing conditions, but the reducing degree of the paleoenvironments of the shales is stronger than that of the mudstones [29]. However, regardless of whether black shales or dark mudstones are more or less generally interbedded with sandstones, the differences in the geochemical characteristics of black shales, dark mudstones and their respective juxtaposed sandstones have been scarcely reported.

In this study, we analyzed the geochemical characteristics of source rocks of the Lower and Middle C7 members (C7-3 and C7-2), which contain a continuous lacustrine sedimentary sequence that was deposited during the evolution of the lake basin. By conducting a series of geochemical analyses including TOC, Rock-Eval pyrolysis yields, bitumen extraction and quantification, and the separation and quantification of saturates, aromatics, resins and asphaltenes, along with biomarker analyses, we aimed to (1) delineate the differences in the bulk geochemical properties among these members and petroleum generation potential; (2) constrain the differences in chemical compositions between black shales, dark mudstones and their respective juxtaposed sandstones; and (3) identify the factors controlling OM accumulation in these formations and the implication for the shale oil potential.

2. Geological Setting

The Ordos Basin is one of the most important large-scale petroliferous basins in China, and it extends across the central and western parts of the country, with an area of approximately 37×10^4 km^2 (Figure 1a) [30]. The basin comprises six tectonic subunits, the northern Yimeng uplift, the southern Weibei uplift, the western fold thrust belt, the Tianhuan depression, the eastern Jinxi flexural-fold belt and the Yishan slope (Figure 1b). The Ordos Basin experienced a marginal ocean basin in the Early Paleozoic, a littoral basin from the Early to Late Paleozoic, a large interior basin from the Late Permian to the Middle Triassic and a para-foreland basin from the Late Triassic to the Early Cretaceous, finally forming the current tectonic framework [31]. In the Late Triassic, the basin evolved to a foreland basin due to collision and integration of the North China Plate and Yangtze Plate related to the Indosinian Movement [32]. During this period, the Ordos Basin deposited a set of fluvial lacustrine sediments with a thickness of about 1300 m, forming the Yanchang Formation [33]. The Upper Triassic Yanchang Formation is the main oil-bearing formation of the basin, and it can be divided into 10 members, namely Chang 10 to Chang 1 (from bottom to top) [34,35]. The Chang 7 members (C7) of the Yanchang Formation are considered to be the main sources of oil for the reservoirs. The C7 members can be further subdivided into the Lower, Middle and Upper Chang 7 (C7-3, C7-2 and C7-1, respectively) subunits, based on sedimentary cycles and lithologies. The study area is located in the Qingcheng area in the southern of the Ordos Basin, belonging to the Yishan slope (Figure 1b). The Yishan slope is a major area of petroleum production in the Ordos Basin.

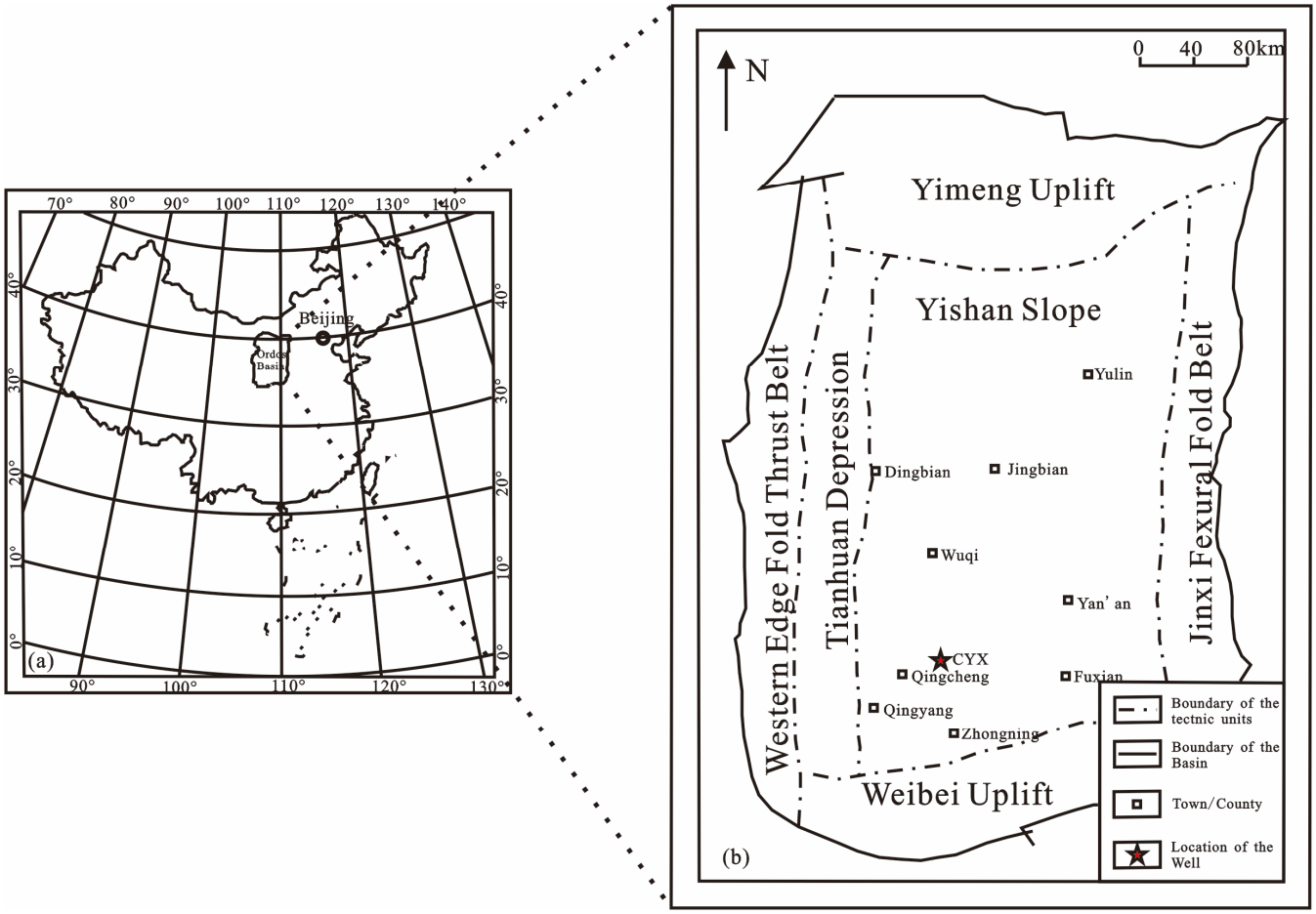

Figure 1. (**a**) Location of the Ordos Basin in China; (**b**) Tectonic units in the Ordos Basin and location of Well CYX (Xu et al. [29]).

3. Materials and Methods

3.1. Sample Description

A total of 22 core samples were collected from C7-3 and C7-2 of the well CYX in the Ordos Basin (Figure 1b). Among these samples, the 13 samples from C7-3 comprised 4 black shales interbedded with sandstones (BSIS), 4 dark mudstones interbedded with sandstones (DMIS) and 5 black shales (BS); the 9 samples from C7-2 included 5 dark mudstones (DM), 2 black shales (BS) and 2 black shales interbedded with sandstones (BSIS).3.2. Bitumen extraction, and separation and quantification of saturates, aromatics, resins and asphaltenes.

Approximately 50 g of rock samples were crushed into powder (80 mesh) and Soxhlet-extracted with chloroform for 72 h. The extracted bitumens were completely dried in a fume hood to be weighed. Asphaltenes were precipitated from the extracts using *n*-hexane, and the precipitated asphaltenes were filtered. Using alumina-silica column chromatography (both activated for 2 h at 400 °C), the hexane-soluble fractions were further separated into saturates, aromatics, and resins. Firstly, saturates were extracted six times using 5 mL *n*-hexane and then aromatics were extracted four times using 5 mL dichloromethane/*n*-hexane (2:1; *v*/*v*). Lastly, resins were extracted using 10 mL anhydrous ethanol and then 10 mL trichloromethane. After the solvent completely evaporated, the saturates, aromatics, resins and asphaltenes were weighed [36].

3.2. Rock-Eval Pyrolysis and TOC

Rock powder of approximately a 120 μm mesh particle size without any pretreatment through solvent extraction was prepared for Rock-Eval 6 pyrolysis analysis. We followed standard heating program conditions (300 °C for 3 min for S_1; 300–550 °C at 25 °C/min

and holding at 550 °C for 1 min for S_2) based on Espitailié et al. [37]. The TOC content was determined using a Leco CS-200 carbon-sulfur analyzer. The samples were pretreated with hydrochloric acid before Leco TOC analysis. The Leco CS-200 carbon-sulfur analyzer was calibrated with standards having known carbon contents.

3.3. GC-MS Analysis

Gas chromatography-mass spectrometry was conducted on saturated and aromatic fractions on a 6890 N gas chromatographer interfaced with a 5973 N mass spectrometer equipped with a 30 m × 0.32 mm i.d. HP-5 column with a 0.25 μm film thickness. For saturated hydrocarbon fraction analysis, the GC oven temperature was initially held at 60 °C for 5 min, ramped from 60 °C to 300 °C at a rate of 4 °C/min and then held at that temperature for 30 min. For aromatic fraction analysis, the initial temperature of the GC oven was set to 80 °C and held at that temperature for 5 min; then, it was ramped at 4 °C/min to a final temperature of 300 °C, with a final hold of 30 min. Helium was used as the carrier gas in both analyses. The electron impact (EI) source was operated at 250 °C and 70 eV. We operated the mass spectrometer over a full-scan mass range of 20 to 750 m/z, and separately in selected ion-monitoring (SIM) mode using m/z 191 and m/z 217. Compound identifications were based on published relative retention times and full-scan mass spectra based on NIST 08 software. The relative abundances of compounds and ratios were determined using peak areas from the extracted ion currents (EICs).

4. Results and Discussion

4.1. Bulk Geochemical Data and Petroleum Generation Potential

The distribution and richness or quality of source rocks determine the petroleum generation potential and thus are crucial in assessing petroleum systems. The richness or quality of source rocks is generally determined by three main factors, i.e., organic matter abundance, kerogen type and thermal maturity.

The TOC (wt%) contents, Rock-Eval data and selected parameters, along with data on fraction compositions are summarized in Table 1 and Figure 2. The TOC contents for the 9 C7-2 samples and 13 C7-3 samples ranged from 1.90 wt% to 11.68 wt%, and 2.53 wt% to 18.21 wt%, respectively. The average TOC content of C7-3 BS was the highest among all the studied samples (16 wt%), followed by that of C7-3 BSIS (15.74 wt%), C7-2 BS (11.52 wt%), C7-2 BSIS (7.83 wt%), C7-3 DMIS (6.33 wt%) and C7-2 DM (3.56 wt%). Previous studies proved that source rocks containing more than 2 wt% TOC can be regarded as very good potential source rocks, and those with over 4 wt% TOC can be regarded as having excellent organic matter richness [38,39]. Thus, most of the samples had very good to excellent organic matter richness, except for one C7-2 DM sample (1.91 wt%).

Other parameters such as S_2 and $S_1 + S_2$ are also crucial for source rock evaluation. The $S_1 + S_2$ values of the studied samples were in the range of 3.01 to 60.42 mg HC/g rock, with an average value of 20.59 mg HC/g (Table 1), suggesting a poor to excellent hydrocarbon generation potential among these samples. Generally, the TOC content and $S_1 + S_2$ share the same depth trend and exhibit a linear relationship, with a Pearson correlation coefficient value of 0.92 (Figures 2 and 3). According to the criteria of source rocks proposed by Peters and Cassa [39], the cross-plot of the TOC content versus $S_1 + S_2$ indicates that C7-3 BS are excellent source rocks; C7-2 BS, C7-2 BSIS and C7-3 BSIS are very good to excellent source rocks; and C7-2 DM and C7-3 DMIS are fair to good source rocks (Figure 3).

Table 1. Rock-Eval pyrolysis data of the source rock samples.

Member	Lithology	Depth (m)	TOC (Wt. %)	S_1 (mg/g)	S_2 (mg/g)	T_{max} (°C)	HI (mg/g)	$S_1 + S_2$ (mg/g)	$S_1/(S_1 + S_2)$
C7-2	Dark mudstone	1996.9	3.42	0.87	2.14	451	63	3.01	0.29
	Dark mudstone	1997.5	4.02	1.54	3.82	438	95	5.36	0.29
	Dark mudstone	1998.5	5.31	0.89	3.3	454	62	4.19	0.21
	Dark mudstone	2002.3	3.17	2.21	5.9	449	186	8.11	0.27
	Dark mudstone	2007.6	1.90	1.64	4.08	453	214	5.72	0.29
	Black shale interbedded sandstone	2010.2	8.54	1.54	3.71	443	43	5.25	0.29
	Black shale	2011.2	11.36	3.08	15.53	449	137	18.61	0.17
	Black shale	2012.4	11.68	2.95	17.17	452	147	20.12	0.15
	Black shale interbedded sandstone	2013.0	7.13	2.59	9.94	454	139	12.53	0.21
C7-3	Dark mudstone interbedded sandstone	2015.1	10.38	3.72	15.6	453	150	19.32	0.19
	Dark mudstone interbedded sandstone	2018.7	8.14	2.16	12.06	451	148	14.22	0.15
	Dark mudstone interbedded sandstone	2021.5	4.25	1.53	4.45	451	105	5.98	0.26
	Dark mudstone interbedded sandstone	2022.1	2.53	0.93	3.1	454	122	4.03	0.23
	Black shale	2023.0	18.21	6.15	54.27	449	298	60.42	0.10
	Black shale	2024.5	16.05	3.94	27.33	451	170	31.27	0.13
	Black shale	2025.4	17.20	6.13	34.32	451	199	40.45	0.15
	Black shale interbedded sandstone	2036.1	18.00	6.27	41.48	451	230	47.75	0.13
	Black shale interbedded sandstone	2037.4	18.18	6.03	37.95	452	209	43.98	0.14
	Black shale interbedded sandstone	2038.3	11.56	2.65	14.05	453	122	16.7	0.16
	Black shale interbedded sandstone	2041.2	15.24	3.15	24.98	451	164	28.13	0.11
	Black shale	2044.3	14.04	3.58	26.31	451	187	29.89	0.12
	Black shale	2046.2	14.51	4.02	23.83	456	164	27.85	0.14

TOC = total organic carbon (Wt.%); S_1 = free hydrocarbons (mg HC/g rock); S_2 = pyrolytic hydrocarbon yield (mg HC/g rock); T_{max} = temperature with maximum hydrocarbon generation; HI = hydrogen index; $S_1 + S_2$ = potential yield (mg HC/g rock); $S_1/S_1 + S_2$= production index.

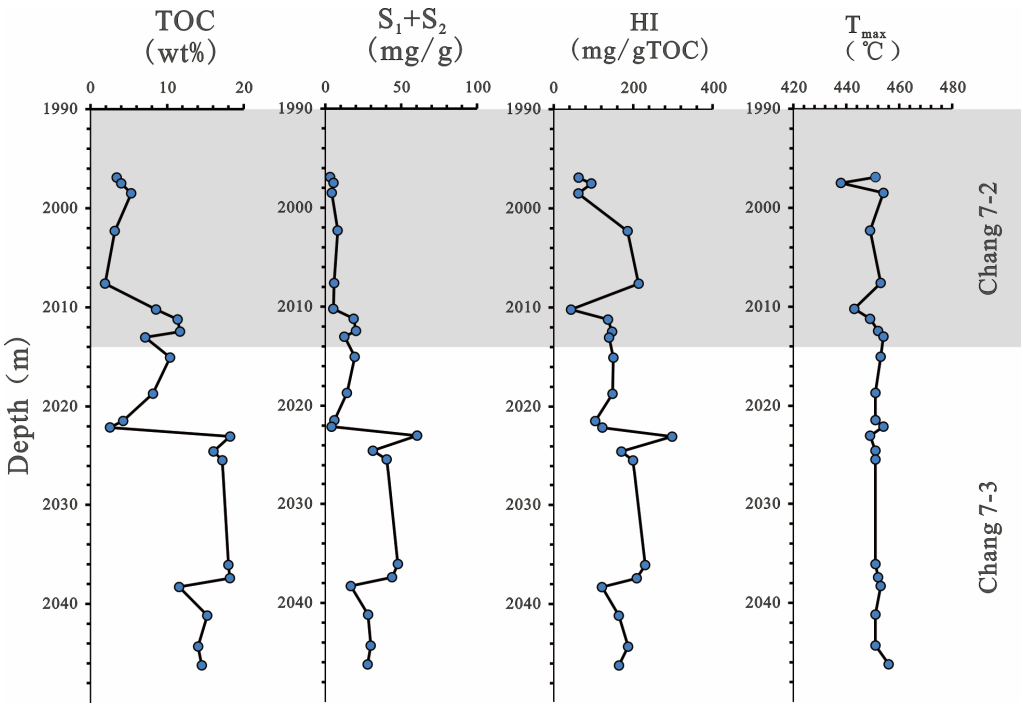

Figure 2. Vertical distribution of total organic carbon (TOC), generative potential ($S_1 + S_2$), hydrogen index and T_{max}.

The kerogen type is another factor that affects the quality of source rocks, which determines the properties and composition of hydrocarbons. The HI values for all the studied samples were generally low, ranging from 43 to 298 mg HC/g TOC; the relatively high values appeared at stages of C7-3 (Figure 2). HI values lower than 200 mg HC/g TOC correspond to Type III kerogens that are mostly composed of woody materials [40]. Therefore, most samples had Type III to mixed Type III/II kerogens. Figure 4 shows the

diagram of HI versus T_{max}. Most of the samples fall in the mature zone of Type II/III kerogens and the Type III area, except for partial C7-3 BS and C7-3 BSIS samples, which belong to Type II kerogens. This suggests that most of the samples are gas-prone source rocks, and only a few samples are oil-prone source rocks. This result is different from that of previous studies, which indicated that Chang 7 shales mainly contain Type II kerogens [28,29]. Xu et al. [29] investigated the shales in different areas of the Ordos Basin, and the HI values of the shales ranged from 177 to 484 mg HC/g TOC. The HI values in this study are distributed in the lower range. Sun et al.'s [28] research on deep-lacustrine shales of the Ordos Basin showed that they had high HI values of 384–576 mg HC/g TOC. There are certain differences in the kerogen types of the shales in different positions of the lake. The study area is located in the area with a thin accumulated thickness of shales, which has a greater terrigenous source input, resulting in poor organic matter types of the shales in this area [28]. However, the kerogen type of the mudstones is relatively consistent with previous studies and shows little difference.

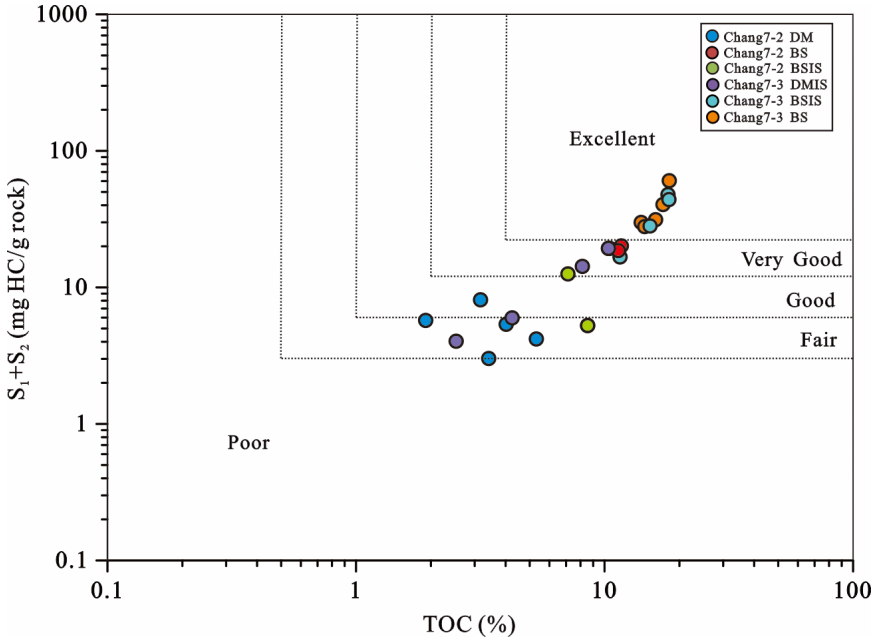

Figure 3. The cross-plot of generative potential (S_1 + S_2) and TOC. DM—dark mudstones; BS—black shales; BSIS—black shales interbedded with sandstones; DMIS—dark mudstones interbedded with sandstones.

Moreover, thermal maturity is also an important proxy for evaluating the quality of source rocks. The T_{max} value is the temperature at which the maximum rate of hydrocarbon generation occurs during Rock-Eval pyrolysis [41] and is often employed as a thermal maturity indicator. The T_{max} values ranged from 438 to 456 °C, with an average value of 450 °C (Figure 2), indicating that all the samples are in the oil-generation window.

In summary, all the studied samples are in the oil-generation window. Most of the samples containing Type III kerogens are gas-prone source rocks, except for partial C7-3 BS and C7-3 BSIS samples with Type II kerogens. Combining the variable TOC contents, the source rocks from C7-3 and C7-2 are fair to excellent source rocks.

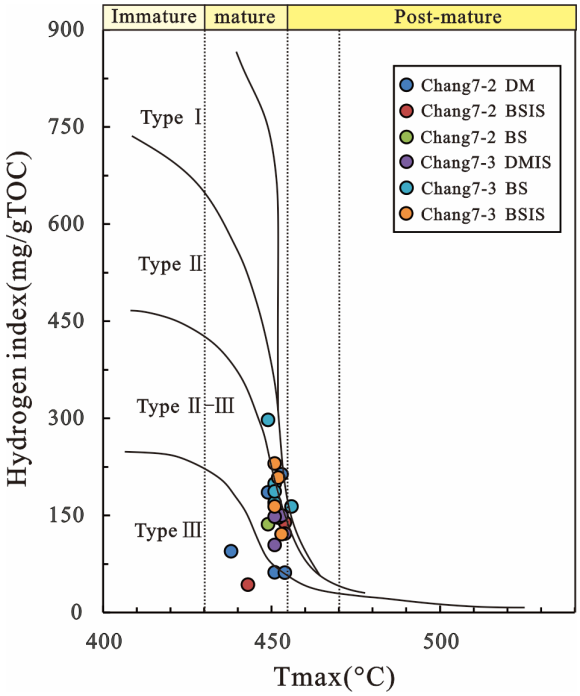

Figure 4. The cross-plot of HI and T_{max} (Hakimi et al. [40]).

4.2. GC-MS Analysis

Biomarkers in oils and source rocks are generally proposed as geochemical indicators in relation to OM input, paleo-depositional environment, and thermal maturity. The molecular composition of saturated hydrocarbons was characterized by *n*-alkanes, isoprenoids and steranes.

4.2.1. *n*-Alkanes

The total ion chromatograms (TICs) of the saturated fractions of selected samples are presented in Figure 5. The carbon number of *n*-alkanes for most of the samples ranged from 12 to 35, following a unimodal distribution maximizing at *n*-C_{18} or *n*-C_{19}. However, some samples show different *n*-alkane distributions, from *n*-C_{12} to *n*-C_{31}, and the maximum peak is mainly *n*-C_{16}. The *n*-alkane fractions of terrestrial higher plants are commonly composed of high-carbon-number *n*-paraffins with an odd-carbon preference [42,43], whereas phytoplankton, algae and microbial lipids are normally composed of lower-molecular-weight *n*-alkanes with an even-carbon predominance in saturated fractions [44,45]. The constituents of the saturated hydrocarbons of the samples included both low (*n*-C_{12} to *n*-C_{21}) and high-molecular-weight *n*-alkanes (*n*-C_{22} to *n*-C_{35} or to *n*-C_{31}) with no even-carbon preference, suggesting a mixture of land plant and aquatic plankton source inputs for the C7-2 and C7-3 samples [46].

However, the proportion of low- and high-molecular-weight *n*-alkanes varied in the saturated fraction of each sample, indicating that the source input of the studied samples changed frequently (Figure 5). The ratios of certain *n*-alkanes generally reflect changes in the contents of terrestrial plants and aquatic hydrocarbons in source rocks or sediments [46]. For example, the wax index is used as an indicator of the relative amounts of terrigenous source input, and a higher ratio indicates a greater terrigenous source input relative to the aquatic source input [47,48].

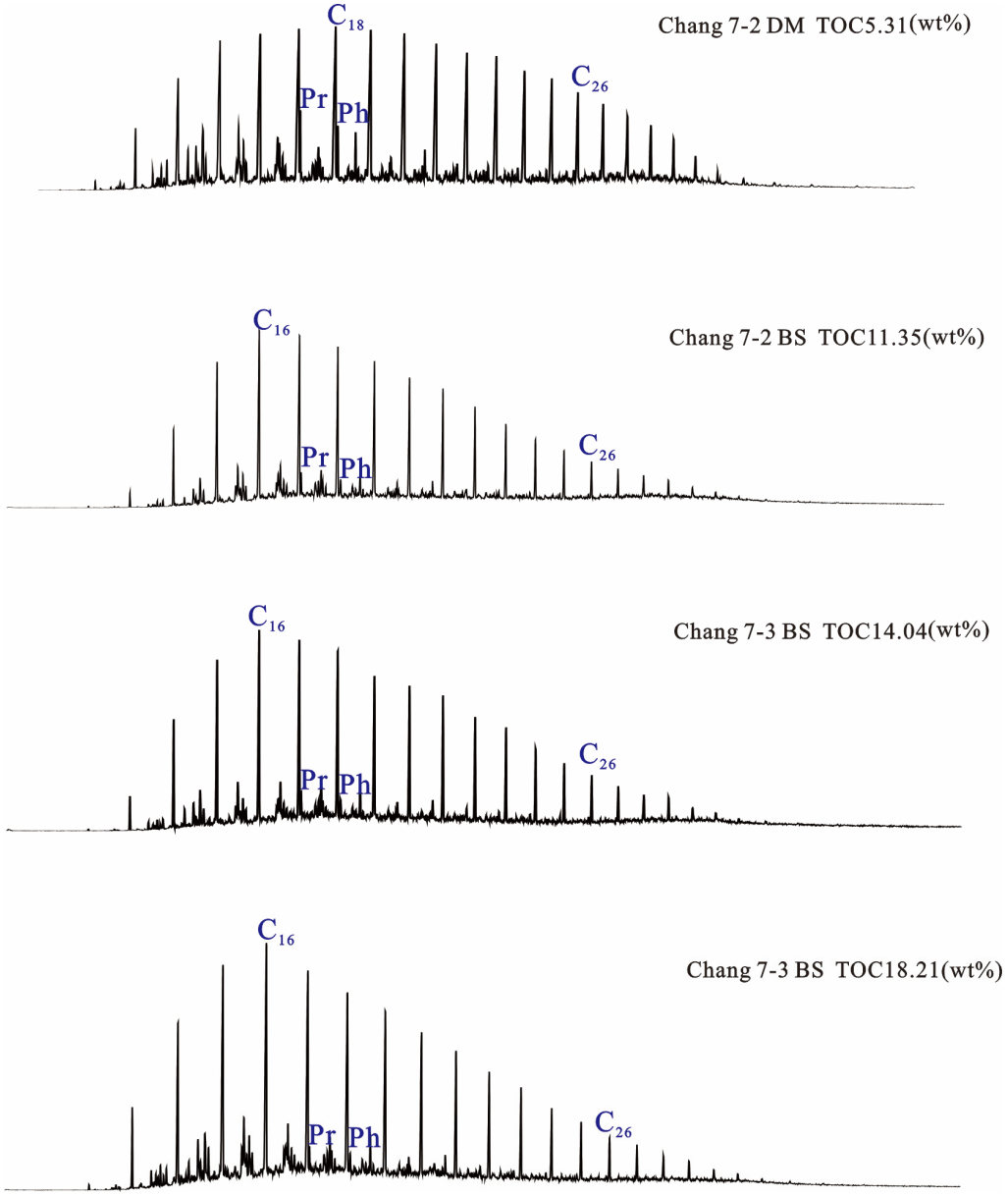

Figure 5. Total ion current gas chromatograms of saturated hydrocarbon fractions for partial samples.

In this study, the ratio of $(nC_{22} - nC_{35})/(nC_{12} - nC_{21})$ was applied as the wax index (Table 2). Figure 6 shows the depth trend of the wax indexes for all the samples. It is clear that the data in the figure vary greatly, implying that the source input changed frequently during the deposition of C7-2 and C7-3. Specifically, the wax indexes for the C7-2 samples were greater than 0.5, except for one C7-2 sample (0.39), ranging from 0.39 to 0.72, with an average value of 0.63, while most of the samples from C7-3 had the wax indexes ranging from 0.29 to 0.63, with an average value of 0.41. Therefore, the wax indexes of the C7-2 samples were higher than those of the C7-3 samples. This indicates that the relative abundance of the terrigenous source input of all the studied samples follows the pattern C7-2 > C7-3.

Table 2. Biomarker ratios for the source rock samples.

Member	Lithology	Depth (m)	wax	Pr/Ph	Pr/nC_{17}	Ph/nC_{18}	TAR	C_{27}/C_{29}
C7-2	Dark mudstone	1996.9	0.71	0.99	0.26	0.26	0.41	1.15
	Dark mudstone	1997.5	0.67	1.09	0.28	0.25	0.38	—
	Dark mudstone	1998.5	0.59	1.05	0.23	0.22	0.30	1.00
	Dark mudstone	2002.3	0.72	1.00	0.32	0.32	0.45	0.99
	Dark mudstone	2007.6	0.70	0.93	0.23	0.24	0.39	0.97
	Black shale interbedded sandstone	2010.2	0.39	0.94	0.10	0.11	0.12	0.91
	Black shale	2011.2	0.32	0.97	0.10	0.10	0.09	0.92
	Black shale	2012.4	0.29	0.92	0.07	0.08	0.05	1.02
	Black shale interbedded sandstone	2013.0	0.63	0.97	0.37	0.37	0.40	0.99
C7-3	Dark mudstone interbedded sandstone	2015.1	0.48	0.94	0.16	0.17	0.22	1.01
	Dark mudstone interbedded sandstone	2018.7	0.35	0.87	0.10	0.12	0.08	1.37
	Dark mudstone interbedded sandstone	2021.5	0.65	0.86	0.16	0.18	0.36	1.10
	Dark mudstone interbedded sandstone	2022.1	0.52	0.90	0.12	0.13	0.24	1.10
	Black shale	2023.0	0.31	1.01	0.08	0.08	0.08	1.10
	Black shale	2024.5	0.36	0.97	0.12	0.13	0.09	1.13
	Black shale	2025.4	0.32	1.03	0.10	0.10	0.08	1.08
	Black shale interbedded sandstone	2036.1	0.32	1.05	0.12	0.12	0.08	0.93
	Black shale interbedded sandstone	2037.4	0.34	0.98	0.10	0.10	0.08	1.15
	Black shale interbedded sandstone	2038.3	0.36	1.06	0.11	0.11	0.09	1.16
	Black shale interbedded sandstone	2041.2	0.33	0.95	0.09	0.10	0.10	1.35
	Black shale	2044.3	0.45	1.09	0.12	0.11	0.19	1.14
	Black shale	2046.2	0.52	1.14	0.13	0.11	0.23	—

wax = $(nC_{22} - nC_{35})/(nC_{12} - nC_{21})$; Pr = pristane; Ph = phytane; TAR = $(C_{27} + C_{29} + C_{31})/(C_{15} + C_{17} + C_{19})$; C_{27}/C_{29} =the ratio of C_{27}/C_{29} regular steranes.

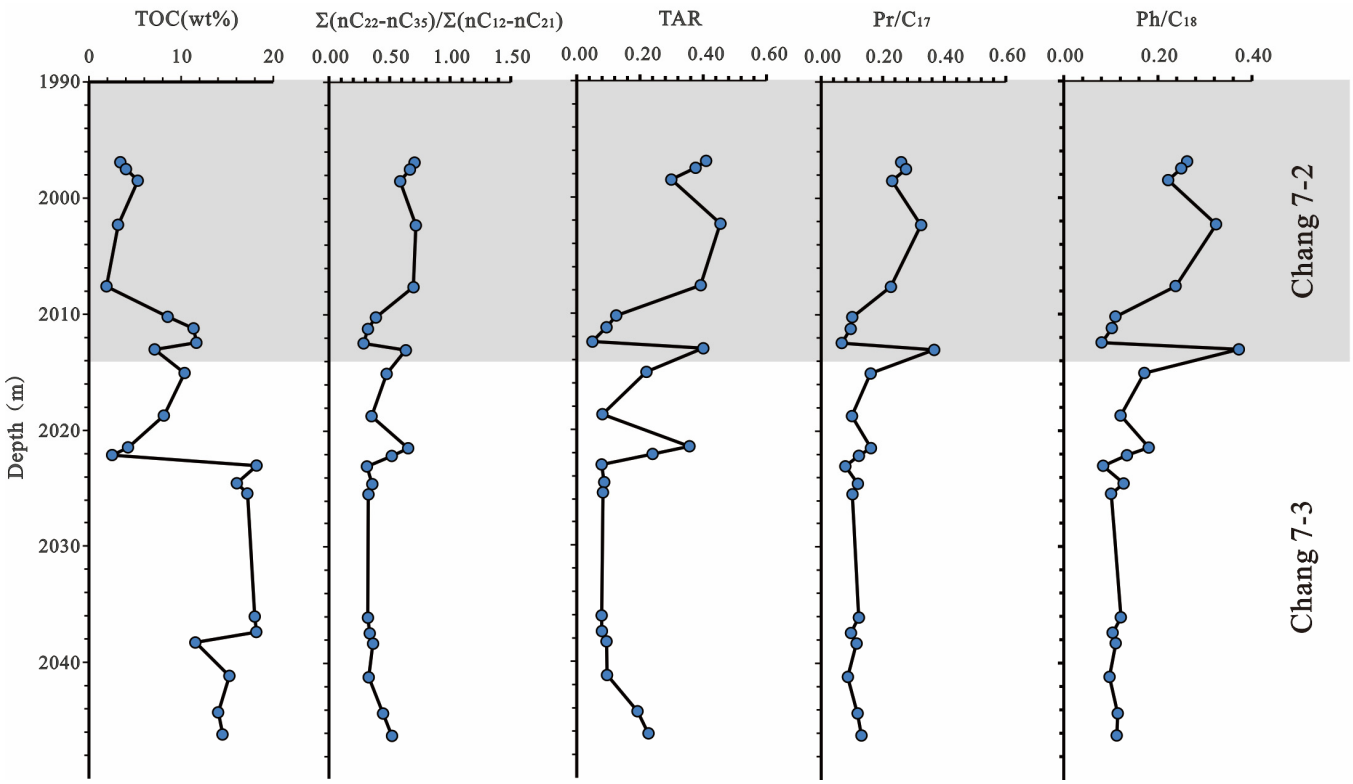

Figure 6. The depth trends of the wax indexe $(nC_{22} - nC_{35})/(nC_{12} - nC_{21})$, TAR $(C_{27} + C_{29} + C_{31})/(C_{15} + C_{17} + C_{19})$, ratios of Pr/C_{17} and ratios of Ph/C_{18} for source rock samples from well CYX.

Additionally, the terrigenous/aquatic ratio (TAR): $(C_{27} + C_{29} + C_{31})/(C_{15} + C_{17} + C_{19})$, can be used as an indicator in terms of the source input [49]. By measuring the vertical

distributions of the TAR, the relative changes in the contribution of land plants versus aquatic flora in source rocks, particularly in young sediments, over geological time can be determined [50]. Figure 6 shows the vertical distributions of the TAR measurements. The TAR varied with the burial depth, indicating that the source input for all the samples is different. Specifically, source rocks from C7-3 had an average TAR (0.15), ranging from 0.08 to 0.36, while source rocks from C7-2 had a higher average TAR (0.29) ranging from 0.05 to 0.45. This suggests that terrigenous source input is on a steady rise from C7-3 to C7-2, which is consistent with the wax index results.

However, both the wax index and TAR are sensitive to secondary processes, such as thermal maturation, and thus must be used with caution [46]. Since high-carbon-number alkanes tend to generate lower-carbon-number alkanes through the process of thermal cracking, a higher thermal maturity results in a lower wax index and TAR. All the samples are in the oil-generation window, but most of the samples share similar thermal maturities, as indicated by the T_{max} values (Table 1 and Figure 2). Given that the source inputs of all the studied samples are similar, the values of the wax index and TAR for the samples should also be similar. However, in fact, C7-2 has a higher wax index and TAR. This further suggests that terrigenous source input is more abundant in C7-2, and that the wax index and TAR can reflect changes in the relative amounts of terrigenous versus aquatic and microbial lipid source inputs in this study.

Interestingly, the wax index and TAR seem to have links with the TOC content. For example, the average TOC content for all the studied samples follows the pattern C7-3 > C7-2, whereas the average wax index and TAR follow the pattern C7-2 > C7-3. This suggests that a high wax index and TAR correspond to a low TOC content, i.e., the wax index and TAR have a negative relationship with the TOC content. Further, the depth trend of both the wax index and TAR for all the samples is the opposite of that of the TOC content in general (Figure 6). This suggests that the contribution of terrigenous source input to the accumulation of OM is limited, while aquatic source input, such as plankton and algae favors the formation of high-TOC-content source rocks. To further elucidate the relationship between the wax index and TAR and TOC content, cross-plots of the wax index and TAR versus TOC were employed (Figure 7). It is clear that the TAR and wax index have a negative relationship with the TOC content, which is consistent with the results in Figure 6.

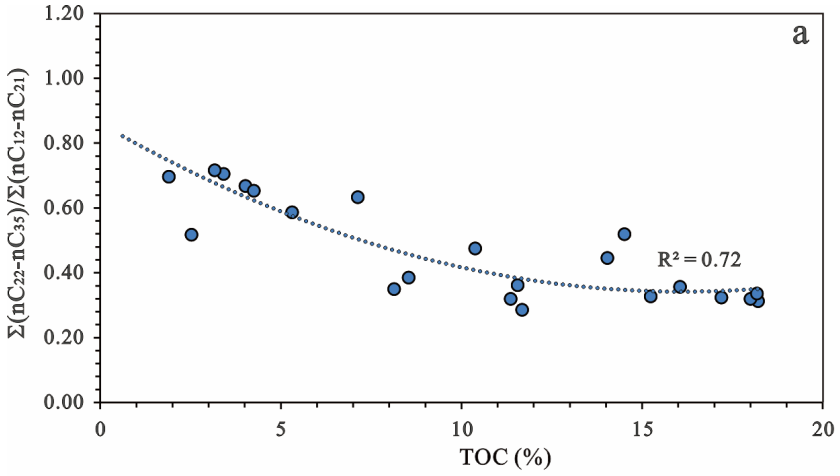

Figure 7. *Cont.*

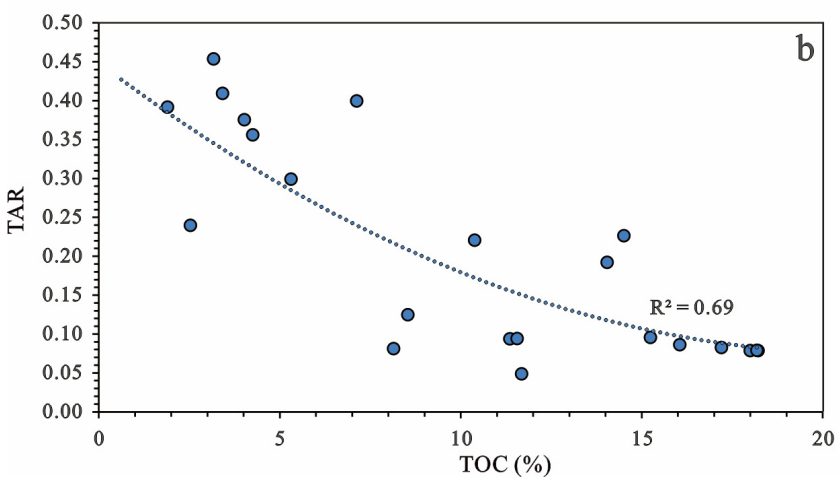

Figure 7. Cross-plots of (**a**) the wax indexes versus TOC contents, and (**b**) TAR versus TOC contents.

4.2.2. Acyclic Isoprenoids

Pristane (Pr) and phytane (Ph) are two common acyclic isoprenoids distributed in sediments and source rocks. Their origins are thought to be related to the degradation of the phytol side chain of chlorophyll [51,52]. Anoxic conditions favor the generation of phytane by the reduction in phytol, while oxic environments promote the oxidation of phytol to yield pristane. Thus, Pr/Ph ratios can be engaged as an indicator to infer the depositional environments [53]. According to previous studies, Pr/Ph < 1 indicates that the source rocks were deposited in anoxic conditions, while Pr/Ph > 1 suggests oxic deposition, and Pr/Ph > 3 is usually detected in coals and thus implies a terrigenous source input under oxic conditions [53,54]. The Pr/Ph ratios of the samples ranged from 0.86 to 1.13 (Table 2), with an average value of 0.99, suggesting all the source rocks were deposited under sub-anoxic to sub-oxic conditions. This is consistent with similar redox environments inferred by Xu et al. [29], but suggests a stronger oxic condition than that of the deep-lacustrine shales [28].

Pr/nC_{17} and Ph/nC_{18} are two parameters controlled by the source input, depositional condition, thermal maturity and biodegradation and thus can be widely used in petroleum correlation studies [55]. Pr/nC_{17} ratios < 0.5 are indicative of open-water conditions, while values greater than 1 suggest inland peat swamps [56,57]. Low Pr/nC_{17} ratios in sediments may be caused by the contribution of microbial lipids or marine algae [58]. Additionally, thermal maturity decreases Pr/nC_{17} and Ph/nC_{18} ratios [59,60], while biodegradation increases the two ratios since aerobic bacteria prefer to consume *n*-alkanes before isoprenoids. The ratios of Pr/nC_{17} and Ph/nC_{18} for all the samples ranged from 0.07 to 0.37, and 0.08 to 0.37 (Table 2), respectively. The low values indicate that the source rocks experienced a high thermal maturity or were deposited in open-water conditions or even both.

Figure 6 shows the vertical measurements of the Pr/nC_{17} and Ph/nC_{18} ratios. It is clear that the depth trend of the two ratios is similar to that of the wax index and TAR, whereas it is the opposite of that of the TOC content in general. Figure 8 shows the cross-plots of Pr/nC_{17} and Ph/nC_{18} versus the wax index and TAR. It is clear that the Pr/nC_{17} and Ph/nC_{18} ratios have a positive relationship with the wax index and TAR. This suggests that the Pr/nC_{17} and Ph/nC_{18} ratios may be controlled by the source input, and that a greater aquatic source input leads to lower Pr/nC_{17} and Ph/nC_{18} ratios. According to Bechtel et al. [58], a low Pr/nC_{17} ratio may be related to the formation of microbial lipids or a contribution of marine algae. The low values in the source rocks of C7-3 may be affected by the enhanced contribution of microbial lipids or aquatic source inputs, such as plankton and algae.

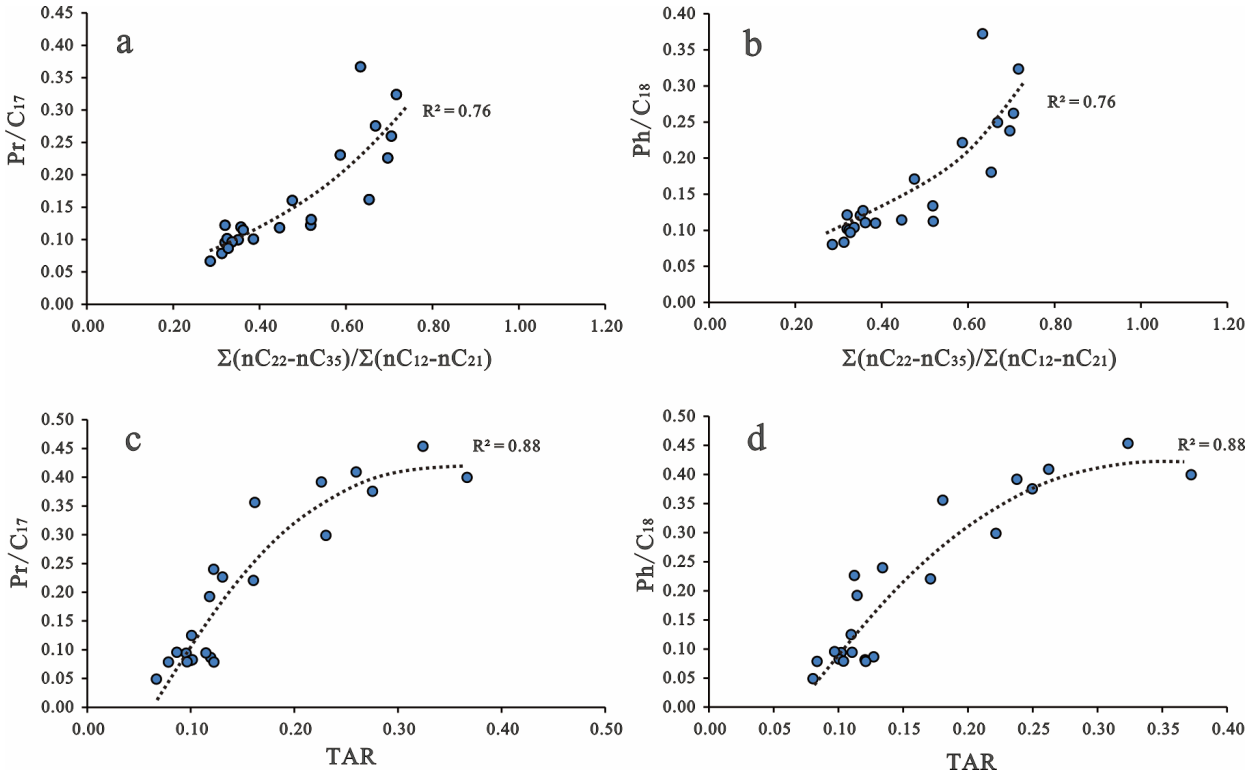

Figure 8. Cross-plots: (**a**) the wax indexes versus Pr/C_{17}; (**b**) the wax indexes versus Ph/C_{18}; (**c**) TAR versus Pr/C_{17}; (**d**) TAR versus Ph/C_{18}.

4.2.3. Steranes

Steranes were observed using the *m*/*z* 217 chromatograms (Figure 9). C_{27} and C_{28} sterols are mainly derived from phytoplankton or algae, while C_{29} sterols are thought to be related to terrigenous source input [61]. The distributions of the C_{27}, C_{28} and C_{29} regular steranes of all the studied samples mainly show V-shaped patterns on the *m*/*z* 217 mass chromatograms (Figure 9). Generally, for most of the samples from C7-2 and C7-3, the concentration of C_{27} regular steranes was slightly higher than that of C_{29} regular steranes.

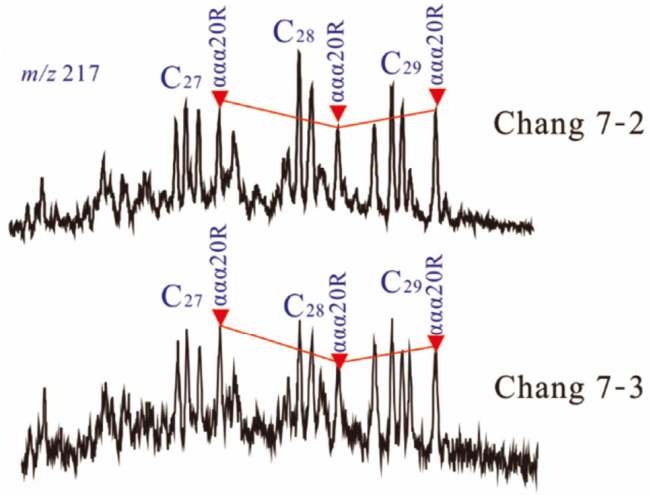

Figure 9. The distribution of regular steranes for partial Chang 7-2 and Chang 7-3 source rocks.

However, the relative abundance of C_{27}, C_{28} and C_{29} regular steranes was variable for all the studied samples. The ratios of C_{27}/C_{29} regular steranes for the samples from C7-2 and C7-3 ranged from 0.91 to 1.15 and 0.93 to 1.37, with an average value of 0.99 and 1.14,

respectively (Table 2). It is noteworthy that the C_{27}/C_{29} ratios seemingly have a positive relationship with the TOC abundance since the average values of both the C_{27}/C_{29} ratios and TOC contents for all the studied samples follow the pattern C7-3 > C7-2 (Figure 10). The C_{27}/C_{29} ratios basically increase with the TOC abundance, indicating that the source input of phytoplankton or algae favors OM accumulation. This is consistent with the results found when analyzing by alkanes and acyclic isoprenoids.

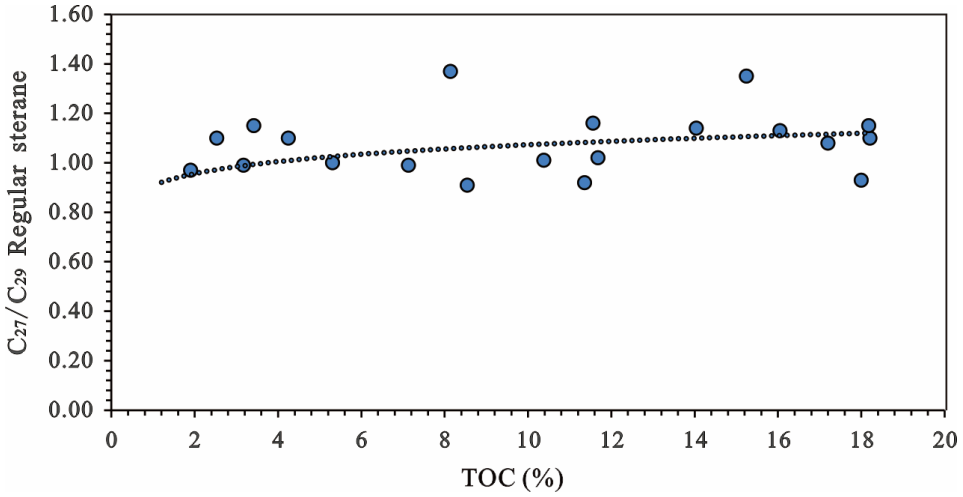

Figure 10. The cross-plot of the ratios of C_{27}/C_{29} regular sterane versus TOC contents.

In summary, the distribution of *n*-alkanes, acyclic isoprenoids and regular steranes varied in all samples. Generally, the average of the wax index, TAR, Pr/nC_{17} and Ph/nC_{18} ratios and relative content of C_{29} regular steranes for source rocks from C7-2 is higher than that of source rocks from C7-3. This suggests that terrigenous source input is more abundant in C7-2, whereas the source input of phytoplankton, algae or microbial lipids is more abundant in C7-3. Moreover, a high TOC content basically corresponds to low wax indexes, TARs and Pr/nC_{17} and Ph/nC_{18} ratios and high C_{27}/C_{29} regular sterane ratios, which suggests that the source input of phytoplankton, algae or microbial lipids is favorable for OM accumulation during the deposition of C7-2 and C7-3.

4.3. Petroleum Migration and Shale Oil Potential

4.3.1. Chemical Composition of Hydrocarbons in Mudstones, Shales and Interbedded Sandstones

A shale oil resource system generally refers to petroleum produced from shales, mudstones or closely associated coarser-grained lithologies, such as interbedded sandstones [62]. Due to the frequent changes in depositional environments and source inputs during the evolution of the Ordos Basin, lithology facies have been altered significantly in lateral and vertical directions even over a short distance [24]. Taking the C7-3 as an example, sandstones are, as a rule, interbedded with shales. Figuring out whether the hydrocarbons in sandstones migrated from juxtaposed shales is one of the prerequisites for shale oil exploration.

Figure 11 shows the distribution of saturated fractions in shales and juxtaposed sandstones. It is clear that saturated hydrocarbons in the interbedded sandstones share a similar distribution pattern with shales, which is independent of the TOC abundance, indicating that hydrocarbons in the sandstones migrated from the adjoining shale source rocks. According to Mackenzie et al. [63], the preferential expulsion of components with lower-carbon-number alkanes over those with higher-carbon-number alkanes was observed in oils expelled from a Type-III source rock. This phenomenon may be related to the kerogen type and has not been observed in source rocks with Type-II kerogens [64–68]. The same constituents of saturate fractions in shales and interbedded sandstones also indicate that there is no preferential expulsion occurred. This further suggests that the expulsion

efficiencies of shale source rocks remain uniform and high throughout the entire molecular range since the expulsion efficiency is believed to be high for good-quality source rocks [69].

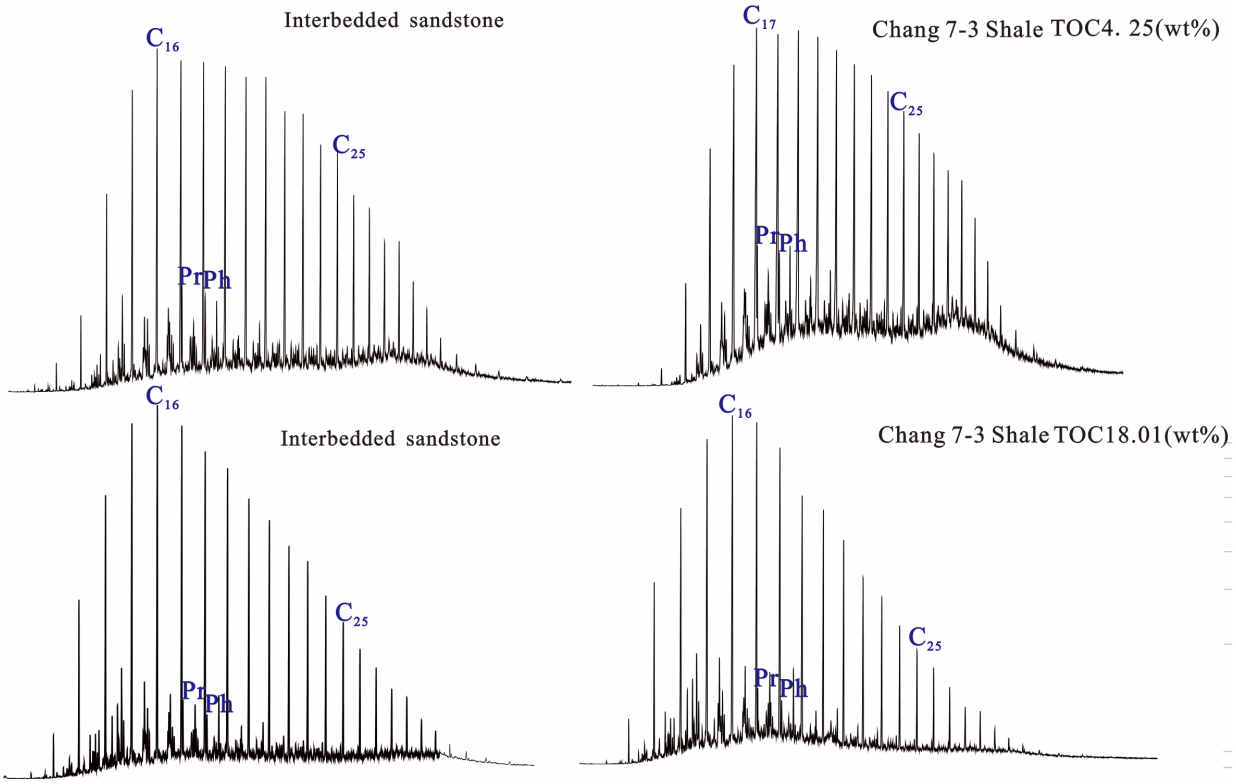

Figure 11. The distribution of saturated fractions in Chang 7-3 shales and juxtaposed sandstones.

Nonetheless, the petroleum compositions were quite different in the shales and interbedded sandstones. Specifically, aromatic and polar fractions were more abundant in the shales than in the juxtaposed sandstones, which were enriched in aliphatic fractions (Figure 12). In addition, the petroleum compositions of all the studied samples were variable. The C7-2 mudstones were dominated by saturates and aromatics, while the C7-2 and C7-3 shales were more enriched in resins and asphaltenes (Figure 12). The contrasting petroleum compositions may be caused by a preferential migration of aliphatic fractions from the organic-rich shales to organic-lean juxtaposed sandstones, which is consistent with the preferential retention of hydrocarbons in the following order: asphaltenes > resins > aromatics > aliphatic, as proposed by Leythaeuser et al. [65]. Two considerable factors are responsible for this phenomenon. First, polar compounds, i.e., asphaltenes and resins, are preferentially adsorbed by kerogen network over apolar compounds, i.e., saturates [70]. Another factor may be that the molecular volume of asphaltenes and resins is relatively too large to migrate. Both of these factors result in a contrasting composition of hydrocarbons in reservoirs and source rocks [1,16,64–68,71]. For instance, the preferential retention of asphaltenes and resins over aromatics and saturates has been observed within the Barnett Shale [67,72].

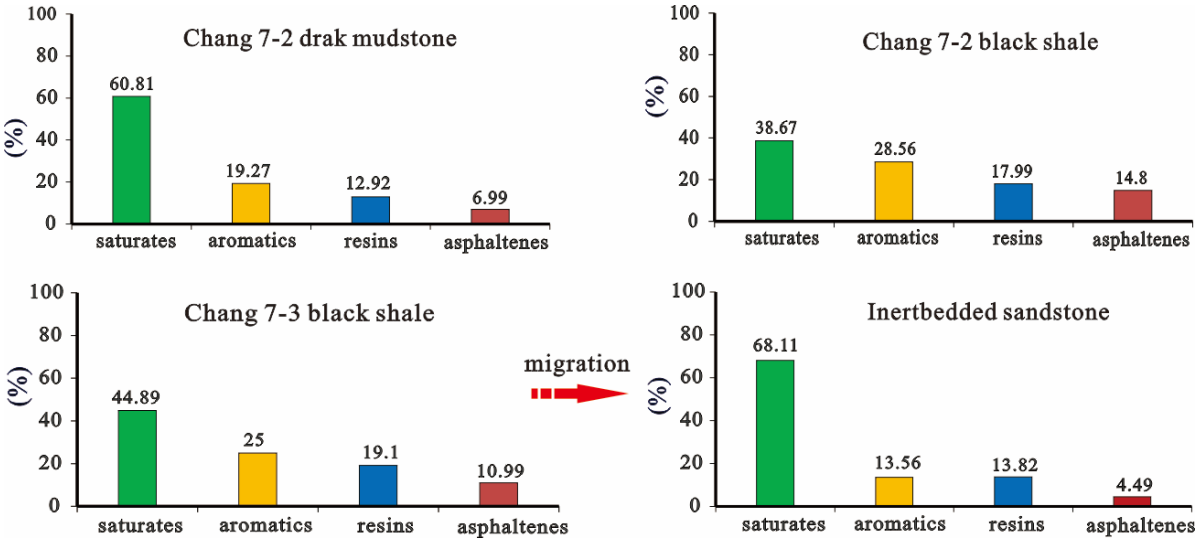

Figure 12. The distribution of saturate, aromatic, resin and asphaltene fractions in partial samples from well CYX.

4.3.2. The Production Index and Oil Saturation Index

The ratio of $S_1/(S_1 + S_2)$ is generally termed the production index and can be applied as a measure of free oil in source rocks and an indicator of migrated oil in sandstones [69]. Figure 13 shows the cross-plot of the production index versus TOC abundance for all the studied samples. Generally, for the samples with TOC > 10%, mainly C7-2 BS, C7-3 BS and BSIS, the production index was low with a narrow change; meanwhile, for those with TOC contents < 5%, mainly partial C7-3 DMIS and C7-2 DM, the production index was relatively high. This suggests that the petroleum in those organic-lean samples may have migrated from source rocks with a high TOC content, such as C7-3 shales, which is consistent with the results observed in previous studies [16,29].

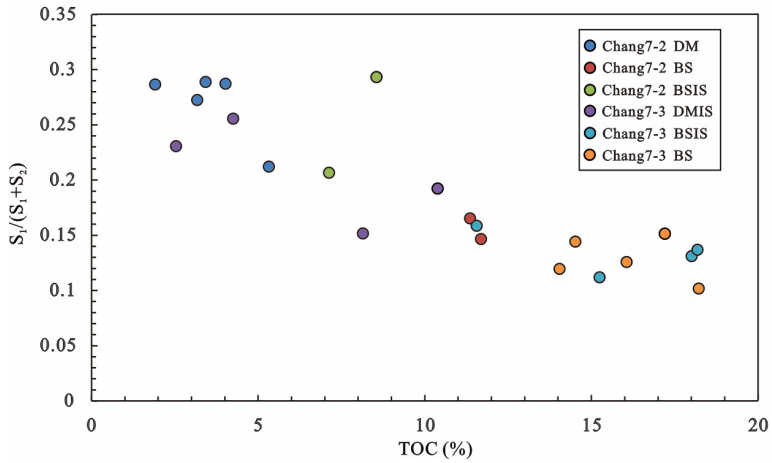

Figure 13. Plot of production index ($S_1/S_1 + S_2$) versus TOC content. The high production index in sandstones with a low TOC content is a result of migrated oil.

The oil saturation index (OSI) is calculated as $S_1/TOC \times 100$ and was proposed by Jarvie [62,73] to identify the degree of oil saturation in source rocks or oil-bearing zones that may hold producible oil. Based on surveying the geochemical characteristics of North American marine shales, Jarvie [62,73] found the "oil crossover" effect, whereby "free" oil can be expelled from shales or mudstones only after overcoming a sorption threshold exerted by minerals, i.e., clay minerals and organic matter network (kerogens), when the OSI exceeds 100 mg/g TOC. However, both the type of OM and the composition of minerals

of lacustrine shales are quite different from those of marine shales. Therefore, this criterion may not be suitable for the evaluation of lacustrine shales. Huang et al. [74] found that the OSI for mudstones and shales of C7 is approximately 70 mg/g TOC. In the cross-plot of S_1 versus TOC (Figure 14), S_1 exhibits a positive relationship with the TOC abundance, indicating that the retention of hydrocarbons in the samples is determined by the richness of OM. Additionaly, it is clear that the OSI for most of the studied samples was lower than 70 mg/g TOC, and only two C7-2 DM exceeded this criterion. Combined with the fact that they are more enriched in aliphatic fractions (Figure 12), C7-2 DM could be considered as a potential "sweet spot" of shale oil. The variations in the richness of OM result in petroleum migrating from organic-rich units to their organic-lean counterparts.

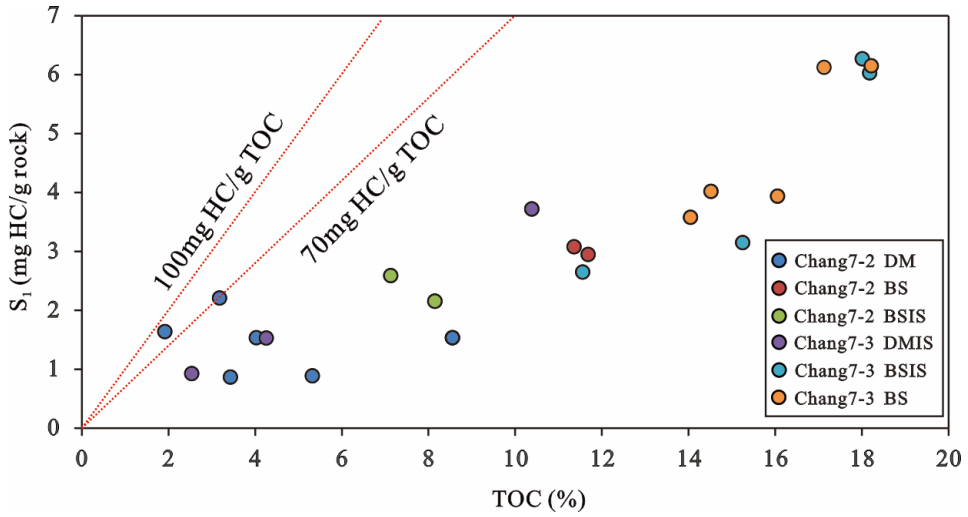

Figure 14. The cross-plot of S_1 versus TOC content for source rocks from well CYX.

5. Conclusions

Based on the systematic analysis of the bulk geochemical characteristics, chemical compositions of hydrocarbons and biomarkers associated with the C7-2 and C7-3 lacustrine mudstones, shales and their juxtaposed interbedded sandstones, the following conclusions can be drawn:

(1) The C7-2 and C7-3 source rocks are thermally mature and have entered into the stage of hydrocarbon generation. The source rocks of C7-2 and most of the samples from C7-3 contain Type III kerogens and mixed Type III/II kerogens and are gas-prone source rocks, except for partial C7-3 BS and C7-3 BSIS, which contain Type II kerogens and are oil-prone source rocks. Most of the C7-3 and C7-2 source rocks have a very good to excellent hydrocarbon generation potential, while the C7-2 DM and C7-3 DMIS samples are fair to good source rocks.

(2) Analyses of the molecular compositions of saturated fractions in shales and interbedded sandstones and the production index demonstrate the migration of petroleum from organic-rich source rocks to their organic-lean counterparts. This process results in aromatic and polar fractions being more abundant in shales, while their juxtaposed sandstones and mudstones are enriched in aliphatic fractions. C7-2 DM could be considered a potential "sweet spot" of shale oil since their OSI was the highest among all the studied samples and they had the richest light aliphatic fractions.

(3) According to the analyses of biomarkers, terrigenous source input is more abundant in C7-2, whereas the source input of phytoplankton, algae or microbial lipids is more abundant in C7-3. Moreover, a high TOC content basically corresponds to low wax indexes, TARs and Pr/nC_{17} and Ph/nC_{18} ratios and high C_{27}/C_{29} regular sterane ratios, which suggests that the source input of phytoplankton, algae or microbial lipids is favorable for OM accumulation.

Author Contributions: Conceptualization, X.M. and W.G.; methodology, L.H. and W.G.; software, Z.R.; validation, X.M. and W.G.; formal analysis, L.H., X.M. and H.T.; investigation, L.H., W.G. and W.H.; data curation, Z.R. and W.H.; writing—original draft preparation, L.H. and W.G.; writing—review and editing, L.H., X.M. and W.G.; supervision, H.T.; funding acquisition, X.M. All authors have read and agreed to the published version of the manuscript.

Funding: This research was funded by the National Natural Science Foundation of China, grant number 41802160.

Data Availability Statement: Not applicable.

Conflicts of Interest: The authors declare no conflict of interest.

References

1. Tissot, B.P.; Welte, D.H. *Petroleum Formation and Occurrence*, 2nd ed.; Springer-Verlag: Berlin/Heidelberg, Germany, 1984.
2. Magoon, L.B.; Dow, W.G. The petroleum system. In *The Petroleum System: From Source to Trap*; Magoon, L.B., Dow, W.G., Eds.; AAPG: Tulsa, OK, USA, 1994; Volume 60, pp. 3–24.
3. Liu, B.; Mastalerz, M.; Schieber, J. SEM petrography of dispersed organic matter in black shales: A review. *Earth Sci. Rev.* **2022**, *224*, 103874. [CrossRef]
4. Zhang, W.; Yang, W.; Xie, L. Controls on organic matter accumulation in the Triassic Chang 7 lacustrine shale of the Ordos Basin, central China. *Int. J. Coal Geol.* **2017**, *183*, 38–51. [CrossRef]
5. Zhao, Y.; Zhang, C.; Lu, J.; Zhu, X.; Li, L.; Si, S. Sedimentary Environment and Model for Organic Matter Enrichment: Chang 7 Shale of Late Triassic Yanchang Formation, Southern Margin of Ordos Basin, China. *Energies* **2022**, *15*, 2948. [CrossRef]
6. Guo, R.; Zhao, Y.; Wang, W.; Hu, X.; Zhou, X.; Hao, L.; Ma, X.; Ma, D.; Li, S. Application of Rare-Earth Elements and Comparison to Molecular Markers in Oil–Source Correlation of Tight Oil: A Case Study of Chang 7 of the Upper Triassic Yanchang Formation in Longdong Area, Ordos Basin, China. *ACS Omega* **2020**, *5*, 22140–22156. [CrossRef] [PubMed]
7. Chen, G.; Wang, N.; Yang, S.; Li, X.; Zhang, P.; Su, Y. Source rock potential of the Upper Triassic Chang 7 member in the western Ordos Basin, China. *J. Pet. Geol.* **2022**, *45*, 395–415. [CrossRef]
8. Cui, J.; Zhu, R.; Li, S.; Qi, Y.; Shi, X.; Mao, Z. Development patterns of source rocks in the depression lake basin and its influence on oil accumulation: Case study of the Chang 7 member of the Triassic Yanchang Formation, Ordos Basin, China. *J. Nat. Gas Geosci.* **2019**, *4*, 191–204. [CrossRef]
9. Tyson, R.V. Sedimentation rate, dilution, preservation and total organic carbon: Some results of a modelling study. *Org. Geochem.* **2001**, *32*, 333–339. [CrossRef]
10. Dong, T.; Harris, N.B.; Ayranci, K. Relative sea-level cycles and organic matter accumulation in shales of the Middle and Upper Devonian Horn River Group, northeastern British Columbia, Canada: Insights into sediment flux, redox conditions, and bioproductivity. *GSA Bull.* **2017**, *130*, 859–880. [CrossRef]
11. Mansour, A.; Wagreich, M. Earth system changes during the cooling greenhouse phase of the Late Cretaceous: Coniacian-Santonian OAE3 subevents and fundamental variations in organic carbon deposition. *Earth Sci. Rev.* **2022**, *229*, 104022. [CrossRef]
12. Mansour, A.; Wagreich, M.; Gentzis, T.; Ocubalidet, S.; Tahoun, S.S.; Elewa, A.M.T. Depositional and organic carbon-controlled regimes during the Coniacian-Santonian event: First results from the southern Tethys (Egypt). *Mar. Pet. Geol.* **2020**, *115*, 104285. [CrossRef]
13. Pedersen, T.F.; Calvert, S.E. Anoxia vs. productivity: What controls the formation of oganic-carbon-rich sediments and sedimentary rocks? *Am. Assoc. Pet. Geol. Bull.* **1990**, *74*, 454–466.
14. Parrish, J.T. Paleogeography of carbon organic-rich rocks and the preservation versus production controversy. In *Paleogeography, Paleoclimate, and Source Rocks*; Huc, A.Y., Ed.; AAPG: Tulsa, OK, USA, 1995; Volume 40, pp. 1–20.
15. Hay, W.W. Paleooceanography of marine organic-carbon-rich sediments. In *Paleoclimate, and Source Rocks*; Huc, A.Y., Ed.; AAPG: Tulsa, OK, USA, 1995; Volume 40, pp. 21–59.
16. Chen, G.; Gang, W.; Chang, X.; Wang, N.; Zhang, P.; Cao, Q.; Xu, J. Paleoproductivity of the Chang 7 unit in the Ordos Basin (North China) and its controlling factors. *Palaeogeogr. Palaeoclimatol. Palaeoecol.* **2020**, *551*, 109741. [CrossRef]
17. Hollander, D.; Behar, F.; Vandernbroucks, M.; Bertrand, P.; Mckenzie, J.A. Geochemical alteration of organic matter in eutrophic Lake Greifen: Implications for the determination of organic facies and the origin of lacustrine source rocks. In *Depositon of Organic Facies*; Huc, A.Y., Ed.; AAPG: Tulsa, OK, USA, 1991; Volume 30, pp. 181–193.
18. Curiale, J.A.; Gibling, M.R. Productivity control on oil shale formation—Mae Sot basin, Thailand. *Org. Chem.* **1994**, *21*, 67–89. [CrossRef]
19. Katz, B.J. A survey of rift basin source rocks. In *Hydrocarbon Habitat in Rift Basins*; Lambiase, J.J., Ed.; Geological Society: London, UK, 1995; Volume 80, pp. 213–240.
20. Gélinas, Y.; Baldock, J.A.; Hedges, J.I. Organic carbon composition of marine sediments: Effect of oxygen exposure on oil generation potential. *Science* **2001**, *294*, 145–148. [CrossRef]
21. Coleman, M.L.; Curtis, D.C.; Irwin, H. Burial rate: A key to source and reservoir potential. *World Oil* **1979**, *188*, 83–92.

22. Ibach, L.E.J. Relationship between sedimentation rate and total organic carbon content in ancient marine sediments. *AAPG Bull.* **1982**, *66*, 170–188.
23. Creaney, S.; Passey, Q.R. Recurring patterns of total organic carbon and source rock quality within a sequence stratigraphy frame work. Am. Assoc. *Pet. Geol. Bull.* **1993**, *77*, 386–401.
24. Yang, H.; Niu, X.; Xu, L.; Feng, S.; You, Y.; Liang, X.; Fang, W.; Zhang, D. Exploration potential of shale oil in Chang7 Member, Upper Triassic Yanchang Formation, Ordos Basin, NW China. *Petrol. Explor. Develop.* **2016**, *43*, 560–569. [CrossRef]
25. Hanson, A.D.; Ritts, B.D.; Moldowan, J.M. Organic geochemistry of oil and source rock strata of the Ordos Basin, north-central China. *AAPG Bull.* **2007**, *91*, 1273–1293. [CrossRef]
26. Tang, X.; Zhang, J.; Jin, Z.; Xiong, J.; Lin, L.; Yu, Y.; Han, S. Experimental investigation of thermal maturation on shale reservoir properties from hydrous pyrolysis of Chang 7 shale, Ordos Basin. *Mar. Pet. Geol.* **2015**, *64*, 165–172. [CrossRef]
27. Jiang, F.; Chen, D.; Wang, Z.; Xu, Z.; Chen, J.; Liu, L.; Hu, Y.; Liu, Y. Pore char-acteristic analysis of a lacustrine shale: A case study in the Ordos Basin, NW China. *Mar. Pet. Geol.* **2016**, *73*, 554–571. [CrossRef]
28. Sun, N.; Chen, T.; Zhong, J.; Gao, J.; Shi, X.; Xue, C.; Swennen, R. Petrographic and geochemical characteristics of deep-lacustrine organic-rich mudstone and shale of the Upper Triassic Chang 7 member in the southern ordos Basin, northern China: Implications for shale oil exploration. *J. Asian Earth Sci.* **2022**, *227*, 105118. [CrossRef]
29. Xu, Z.J.; Liu, L.F.; Liu, B.; Wang, T.G.; Zhang, Z.H.; Wu, K.J.; Feng, C.Y.; Dou, W.C.; Wang, Y.; Shu, Y. Geochemical characteristics of the Triassic Chang 7 lacustrine source rocks, Ordos Basin, China: Implications for paleoenvironment, petroleum potential and tight oil occurrence. *J. Asian Earth Sci.* **2019**, *178*, 112–138. [CrossRef]
30. Yang, H.; Zhang, W.; Wu, K.; Li, S.; Peng, P.; Qin, Y. Uranium enrichment in lacustrine oil source rocks of the Chang 7 member of the Yanchang Formation, Ordos Basin, China. *J. Asian Earth Sci.* **2010**, *39*, 285–293. [CrossRef]
31. Yang, J.J. *Tectonic Evolution and Oil-Gas Reservoirs Distribution in Ordos Basin*; Petroleum Industry Press: Beijing, China, 2002; pp. 36–37. (In Chinese)
32. Liu, C.Y.; Zhao, H.G.; Zhao, J.F.; Wang, J.Q.; Zhang, D.D.; Yang, M.H. Temporospatial coordinates of evolution of the Ordos basin and its mineralization responses. *Acta Geol. Sin.* **2008**, *82*, 1229–1243, (In Chinese with an English abstract).
33. Deng, X.Q.; Lin, F.X.; Liu, X.Y.; Pang, J.L.; Lv, J.W.; Li, S.X.; Liu, X. Discussion on relationship between sedimentary evolution of the Triassic Yanchang Formation and the Early Indosinian Movement in Ordos Basin. *J. Palaeogeogr.* **2008**, *10*, 159–166, (In Chinese with English abstract).
34. Yang, R.; Jin, Z.; Van Loon, T.; Han, Z.; Fan, A. Climatic and tectonic controls of lacustrine hyperpycnite origination in the Late Triassic Ordos Basin, central China: Implications for unconventional petroleum development. *AAPG Bull.* **2017**, *101*, 95–117. [CrossRef]
35. Zou, C.; Wang, L.; Li, Y.; Tao, S.; Hou, L. Deep-lacustrine transformation of sandy debrites into turbidites, Upper Triassic, Central China. *Sediment. Geol.* **2012**, *265–266*, 143–155. [CrossRef]
36. *SY/T 5119-2008*; Analysis Method for Frctions of Rock Extrct and Crude Oil. China Petroleum Standardization Committee: Beijing, China, 2008. (In Chinese)
37. Espitalié, J.; Deroo, G.; Marquis, F. La pyrolyse Rock-Eval et ses applications. *Rev. Inst. Fr. Pét.* **1985**, *40*, 755–784. [CrossRef]
38. Peters, K.E. Guidelines for evaluating petroleum source rock using programmed pyrolysis. *AAPG Bull.* **1986**, *70*, 318–329.
39. Peters, K.E.; Cassa, M.R. Applied source rock geochemistry. In *The Petroleum System—From Source to Trap*; Magoon, L.B., Dow, W.G., Eds.; AAPG: Tulsa, OK, USA, 1994; Volume 60, pp. 93–120.
40. Hakimi, M.H.; Abdulla, W.H. Source rock characteristics and hydrocarbon generation modelling of Upper Cretaceous Mukalla Formation in the Jiza-Qamar Basin, Eastern Yemen. *Mar. Pet. Geol.* **2014**, *51*, 100–116. [CrossRef]
41. Burnham, A.K.; Sweeney, J.J. A chemical kinetic model of vitrinite maturation and reflectance. *Geochim. Cosmochim. Acta* **1989**, *53*, 2649–2657. [CrossRef]
42. Clark, R.C.; Blumer, M. Distributions of n-paraffins in marine organisms and sediments. *Limnol. Oceanogr.* **1967**, *12*, 79–87. [CrossRef]
43. Blumer, M.; Guillard, R.R.L.; Chase, T. Hydrocarbons of marine phytoplankton. *Mar. Biol.* **1971**, *8*, 183–189. [CrossRef]
44. Matsuda, H.; Koyama, T. Early diagenesis of fatty acids in lacustrine sediments-II. A statistical approach to changes in fatty acid composition from recent sediments and some source materials. *Geochim. Cosmochim. Acta* **1977**, *41*, 1825–1834. [CrossRef]
45. Cranwell, P.A. Diagenesis of free and bound lipids in terrestrial detritus deposited in a lacustrine sediment. *Org. Geochem.* **1981**, *3*, 79–89. [CrossRef]
46. Peters, K.E.; Walters, C.C.; Moldowan, J.M. *The Biomarker Guide: Biomarkers and Isotopes in the Environment and Human History*, 2nd ed.; Cambridge University Press: New York, NY, USA, 2005.
47. Hedberg, H.D. Significance of high–wax oils with respect to genesis of petroleum. *AAPG Bull.* **1968**, *52*, 736–750.
48. Connan, J.; Cassou, A.M. Properties of gases and petroleum liquids derived from terrestrial kerogen at various maturation levels. *Geochem. Cosmochim. Acta* **1980**, *44*, 1–23. [CrossRef]
49. Bourbonniere, R.A.; Meyers, P.A. Sedimentary geolipid records of historical changes in the watersheds and productivities of Lakes Ontario and Erie. *Limnol. Oceanogr.* **1996**, *41*, 352–359. [CrossRef]
50. Meyers, P.A. Organic geochemical proxies of paleooceanographic, paleolimnlogic, and paleoclimatic processes. *Org. Geochem.* **1997**, *27*, 213–250. [CrossRef]
51. Brooks, J.D.; Gould, K.; Smith, J.W. Isoprenoid hydrocarbons in coal and petroleum. *Nature* **1969**, *222*, 257–259. [CrossRef]

52. Powell, T.G.; McKirdy, D.M. Relationship between ratio of pristane to phytane, crude oil composition and geological environment in Australia. *Nature* **1973**, *243*, 37–39. [CrossRef]
53. Didyk, B.M.; Simoneit, B.R.T.; Brassell, S.C.; Eglinton, G. Organic geochemical indicators of paleoenvironmental conditions of sedimentation. *Nature* **1978**, *272*, 216–222. [CrossRef]
54. Sofer, Z. Stable carbon isotope compositions of crude oils: Application to source depositional environments and petroleum alteration. *AAPG Bull.* **1984**, *68*, 31–49.
55. Peters, K.E.; Clutson, M.J.; Robertson, G. Mixed marine and lacustrine input to an oil-cemented sandstone breccia from Brora, Scotland. *Org. Geochem.* **1999**, *30*, 237–248. [CrossRef]
56. Lijmbach, G.M. On the origin of petroleum. In Proceedings of the 9th World Petroleum Congress, London, UK, 11 May 1975.
57. Amijaya, H.; Schwarzbauer, J.; Littke, R. Organic geochemistry of the Lower Suban coal seam, South Sumatra Basin, Indonesia: Palaeoecological and thermal metamorphism implications. *Org. Geochem.* **2006**, *37*, 261–279. [CrossRef]
58. Bechtel, A.; Gratzer, R.; Sachsenhofer, R. Chemical characteristics of Upper Cretaceous (Turonian) jet of the Gosau Group of Gams/Hieflau (Styria, Austria). *Int. J. Coal Geol.* **2001**, *46*, 27–49. [CrossRef]
59. Ten Haven, H.L.; de Leeuw, J.W.; Rullkötter, J.; Sinninghe Damsté, J.S. Restricted utility of the pristane/phytane ratio as a palaeoenvironmental indicator. *Nature* **1987**, *330*, 641–643. [CrossRef]
60. Hunt, J.M. *Petroleum Geochemistry and Geology*, 2nd ed.; W. H. Freeman: New York, NY, USA, 1996.
61. Huang, W.Y.; Meinschein, W.G. Sterols as ecological indicators. *Geochim. Cosmochim. Acta* **1979**, *43*, 739–745. [CrossRef]
62. Jarvie, D.M. Shale resource systems for oil and gas: Part 2—Shale-oil resource systems. In *Shale Reservoirs—Giant Resources for the 21st Century*; Breyer, J.A., Ed.; AAPG: Tulsa, OK, USA, 2012; Volume 97, pp. 89–119.
63. Mackenzie, A.S.; Leythaeuser, D.; Schaefer, R.G. Expulsion of petroleum hydrocarbons from shale source rocks. *Nature* **1983**, *301*, 506–509. [CrossRef]
64. Leythaeuser, D.; Radke, M.; Schaefer, R.G. Efficiency of petroleum expulsion from shale source rocks. *Nature* **1984**, *311*, 745–748. [CrossRef]
65. Leythaeuser, D.; Schaefer, R.G.; Radke, M. Geochemical effects of primary migration of petroleum in Kimmeridge source rocks from Brae field area, North Sea. I: Gross composition of C15+-soluble organic matter and molecular composition of C15+-saturated hydrocarbons. *Geochim. Cosmochim. Acta* **1988**, *52*, 701–713. [CrossRef]
66. Wilhelms, A.; Larter, S.R.; Leythaeuser, D.; Dypvik, H. Recognition and quantification of the effects of primary migration in a Jurassic clastic source-rock from the Norwegian continental shelf. *Org. Geochem.* **1990**, *16*, 103–113. [CrossRef]
67. Han, Y.; Mahlstedt, N.; Horsfield, B. The Barnett Shale: Compositional fractionation associated with intraformational petroleum migration, retentioin, and expulsion. *AAPG Bull.* **2015**, *99*, 2173–2202. [CrossRef]
68. Zou, C.; Pan, S.; Horsfield, B.; Yang, Z.; Hao, S.; Liu, E.; Zhang, L. Oil retention and intrasource migration in the organic-rich lacustrine Chang 7 shale of the Upper Triassic Yanchang Formation, Ordos Basin, Central China. *AAPG Bull.* **2019**, *103*, 2627–2663. [CrossRef]
69. Zhang, T.; Wang, X.; Zhang, J.; Sun, X.; Milliken, K.; Ruppel, S.; Enriquez, D. Geochemical evidence for oil and gas expulsion in Triassic lacustrine organic-rich mudstone, Ordos Basin, China. *Interpretation* **2017**, *5*, SF41–SF61. [CrossRef]
70. Sandvik, E.I.; Young, W.A.; Curry, D.J. Expulsion from hydrocarbon sources: The role of organic absorption. *Org. Geochem.* **1992**, *19*, 77–87. [CrossRef]
71. Littke, R.; Leythaeuser, D.; Radke, M.; Schaefer, R.G. Petroleum generation and migration in coal seams of the Carboniferous Ruhr Basin, northwest Germany. *Org. Geochem.* **1990**, *16*, 247–258. [CrossRef]
72. Jarvie, D.M.; Claxton, B.; Henk, B.; Breyer, J. Oil and shale gas from Barnett Shale, Ft. Worth Basin, Texas. In Proceedings of the AAPG National Convention, Denver, CO, USA, 3–6 June 2001.
73. Jarvie, D.M. Components and processes affecting producibility and commerciality of shale resource systems. *Geol. Acta* **2014**, *12*, 307–325.
74. Huang, Z.; Hao, Y.; Li, S.; Wo, Y.; Sun, D.; Li, M.; Chen, J. Oil-bearing potential, mobility evaluation and significance of shale oil in Chang 7 shale system in the Ordos Basin: A case study of Well H317. *Geol. China* **2020**, *47*, 210–219. (In Chinese with English abstract).